7 Network Synchronization

7.1 Introduction

The term *synchronization* is bound with the name Christiaan Huygens (14 April 1629 – 8 July 8 1695), a Dutch mathematician, astronomer and physicist. Huygens worked on the construction of accurate clocks, suitable for naval navigation, over a long period of his lifetime. His invention, the pendulum clock, was a breakthrough in timekeeping, which was patented in 1657. Then, in 1658, he published a book entitled Horologium on this subject. The most important work of Huygens relating to the concept of synchronization was his observation that two pendulums mounted on the same beam would come to swing in perfectly opposite directions, a phenomenon he referred to as odd sympathy.

Another interesting discovery was the observation of fireflies' synchronous flashing by another Dutch, a tourist named Kempfer. When he traveled through the River Naenam in Thailand in 1680, Kempfer found that those little insects could flash together fairly accurately in time.

If attention is paid, one can easily find many synchronization phenomena in different forms in nature as well as man-made systems. For example, an audience expresses appreciation for a good performance by its applause: the tumultuous applause can transform itself into waves of synchronized clapping quickly and this synchrony can also disappear and then reappear several times during the applause. This common social harmony and its generation mechanism may be studied from a complex dynamics point of view [1]. The rhythm in the human heart certainly is another well-known incident. In computer science, especially in parallel computing, synchronization means the coordination of simultaneous threads or processes to complete a task of obtaining a correct runtime order while avoiding unexpected race conditions. There are many types of synchronizations there: barrier, lock/semaphore, non-blocking synchronization, synchronous communication operations, and file synchronization, and so on. There are simply too many examples to list. In fact, in science and technology, synchronization has become a focal subject for study today [2,3].

Yet, synchronization can be harmful. On June 10, year 2000, when the London Millennium Footbridge over the River Thames was first opened to the public, thousands of people walked on it for celebration but unexpectedly lateral vibration (resonant structural response) caused this 690-ton steal bridge to sway severely. This swaying motion earned it a nickname the Wobbly Bridge afterwards. Although the resonant vibrational modes have been well understood in bridge design after the famous event of collapse of the Tacoma Narrows Bridge in 1940, not much attention had been given to pedestrian-excited lateral motion, which was responsible for the big vibration of the millenium bridge. An extensive analysis was conducted thereafter, but it took more than one year and costed about 5-million pounds to finally fix the problems and then re-open the bridge on February 22, 2002.

Internet is another phenomenal example for which synchronization could be harmful. In the Internet, many apparently-independent periodic processes such as routers can inadvertently become synchronized. In particular, the synchronization of periodic routing messages can emerge, which has a harmful effect on other network traffics. Notably, the transition from unsynchronized to synchronized traffic is not a gradual degradation but has a very abrupt phase transition where the addition of a single router can literally convert a completely unsynchronized traffic stream into a completely synchronized one. The danger is that this kind of inadvertent synchronization of periodic processes is likely to become an increasing problem in the Internet [4].

Research reveals that all these seemingly independent events of synchronizations can be described under a unified mathematical framework. Suppose that each individual in a population is a dynamical system oscillating periodically and they are connected as a network. Winfree [5] showed that if each oscillator is strongly coupled with its finitely many neighbors then the amplitudes of these oscillators may be neglected thereby transforming the concerned issue into a phase synchronization problem. From this point of view, by completely ignoring oscillatory amplitudes, Kuramoto [6] further suggested that a network of finitely many coupled oscillators could be described by a simple phase equation, no matter how weak the coupling strength is among them. This formulation facilitates the discussion of the synchronization problem in a finite population of connected oscillators. Since these earlier investigations, various synchronization phenomena on networks have evoked a lot of interests in theoretical as well as practical research studies. In the last century, the main research efforts were focused on regular networks, such as Coupled Map Lattices (CML) [7] and Cellular Neural Networks (CNN) [8]. This kind of simplification on the network structures may have the advantage of studying only the complex dynamics caused by the nonlinearity of the individual systems by ignoring the effects of the complex network topologies. However, network topology certainly has significant effects on the network dynamics particularly synchronous behaviors. For example, as intuitively clear, a strong enough coupling strength can lead to the synchrony of a network [9], but this does not help explain why a weakly coupled network still have very strong tendency towards synchronization. One answer was revealed by the recent discoveries of small-world and scale-free features of various complex network topologies, which have dragged increasing attention to the relationship between the network topology and network synchronous behaviors [9-42, 49-54, and references therein].

7.2 Complete Synchronization of Continuous-Time Networks

A general continuous-time dynamical network and its synchronization problem can be formulated as follows.

Consider a network of N identical nodes, in which node i is described by

$$\dot{x}_i = f(x_i) - c\sum_{j=1}^{N} a_{ij} H(x_j), \quad i = 1,2,...,N \tag{7-1}$$

where $x_i = \left[x_i^{(1)}, x_i^{(2)}, \cdots, x_i^{(n)}\right]^T \in R^n$ is the state vector, constant $c > 0$ is the coupling

strength, $H: R^n \to R^n$ is the *inner coupling* function among different components of a state vector, and $A = [a_{ij}] \in R^{N\times N}$ is the *outer coupling* matrix, which describes an undirected and unweighted network topology, satisfying the following conditions: if there is a connection between node i and node j, for $i \neq j$, then $a_{ij} = a_{ji} = 1$; otherwise, $a_{ij}a_{ji} = 0$, for $i \neq j$; and the diagonal elements are defined by

$$a_{ii} = -\sum_{\substack{j=1\\ j\neq i}}^{N} a_{ij} = -\sum_{\substack{j=1\\ j\neq i}}^{N} a_{ji} = -k_i, \qquad i = 1, 2, \cdots, N \tag{7-2}$$

where k_i is the degree of node i, which is referred to as the *diffusive condition*, i.e., $\sum_j a_{ij} = 0$, for all $i = 1,2,...,N$, describing a kind of energy-balance situation.

Clearly, when all nodes have the same states, i.e., when $x_j \equiv x$ for all $j = 1,2,...,N$, the summation term on the right-hand side of (7-1) vanishes.

Recall from the graph theory studied in Chapter 2 that the matrix $L \equiv -A$ is a Laplacian matrix. If the network is wholly connected without separate sub-nets, then the matrix A is an irreducible matrix, i.e., it cannot be reduced to an upper-triangular form by simultaneous row-column permutations. Thus, by elementary matrix theory, matrix A has a zero eigenvalue of multiplicity 1, associated with the normalized right eigenvector $\frac{1}{\sqrt{N}}[1,1,\cdots,1]^T$, and the other eigenvalues of matrix A are all negative:

$$0 = \mu_1 > \mu_2 \geq \cdots \geq \mu_N \tag{7-3}$$

while the Laplacian matrix $L = -A$ has eigenvalues

$$0 = \lambda_1 < \lambda_2 \leq \cdots \leq \lambda_N \tag{7-4}$$

with $\lambda_i = -\mu_i$, $i = 1,...,N$. In both cases, the set of corresponding n-dimensional right eigenvectors of all the non-zero eigenvalues span an $(N-1)n$-dimensional subspace, transversal to the right eigenvector vector $\frac{1}{\sqrt{N}}[1,1,\cdots,1]^T$ of the zero eigenvalue.

The eigenvalues of the Laplacian matrix $L = -A$ will be used more frequently in the following.

Definition 7.1 If

$$x_1(t) \to x_2(t) \to \cdots \to x_N(t) \text{ as } t \to \infty$$

or, more formally, if

$$\lim_{t\to\infty} \|x_i(t) - x_j(t)\| = 0 \text{ for all } i, j = 1,2,...,N \tag{7-5}$$

where $\|\cdot\|$ is the Euclidean norm, then the network (7-1) is said to achieve *complete* (*asymptotic*) *synchronization*. Moreover,

$$x_1 = x_2 = \cdots = x_N \tag{7-6}$$

is referred to as the *synchronization manifold* in the state space R^n.

It can be seen that to achieve complete synchronization of network (7-1) is equivalent to guarantee its synchronization manifold (7-6) be an *invariant synchronization manifold*, or in other words, to guarantee that its synchronization manifold (7-6) be (*asymptotically*) *stable*, in the following sense: for all network orbits in the state space R^n, if they are moving to be close to this synchronization manifold then they will be attracted to the manifold and, furthermore, if they have entered the manifold then they will be trapped inside forever.

For practical reasons, one usually expects or requires that all the synchronized orbits can converge to a certain desired state, for example, a solution orbit of the node system. Denote this desired orbit by $s(t) \in R^n$, and slightly change the objective, to achieve

$$x_1(t) \to x_2(t) \to \cdots \to x_N(t) \to s(t) \text{ as } t \to \infty$$

or, more formally,

$$\lim_{t\to\infty} \|x_i(t) - s(t)\| = 0 \text{ for all } i = 1,2,...,N \tag{7-7}$$

If one takes the time limit on both sides of (1), and assumes that the network is indeed synchronized to a constant state s, then due to the diffusive coupling condition of the network, one has

$$\dot{s} = f(s) \tag{7-8}$$

Here, since s is a constant vector, one has $\dot{s} = 0$, so $f(s) = 0$, namely, this s is an equilibrium of the node system.

It can be verified that the right eigenvector vector $\frac{1}{\sqrt{N}}[1,1,\cdots,1]^T$ of the zero eigenvalue in (7-3) or (7-4) corresponds to the *invariant synchronization manifold* of network (7-1).

Note that the $(N-1)n$-dimensional subspace transversal to the right eigenvector vector $\frac{1}{\sqrt{N}}[1,1,\cdots,1]^T$ of the zero eigenvalue is

$$\Theta = \left\{ x = \left[x_1^T, x_2^T, \cdots, x_N^T\right]^T \in R^{nN} : \quad \sum_{j=1}^{N} \xi_j x_j = 0 \right\}$$

where $[\xi_1, \xi_2, \cdots, \xi_N]^T$ is the left eigenvector of the zero eigenvalue of matrix A. By nature, the synchronization of network (7-1) is equivalent to that the projections of all the network states $x_1(t), x_2(t), \cdots, x_N(t)$ on Θ asymptotically converge to zero [41].

7.2.1 Complete Synchronization of General Continuous-Time Networks

Linearizing equation (7-1) at the synchronized state $s(t)$ and then letting ξ_i be the variation of the state vector of node i lead to

$$\dot{\zeta}_i = Df(s)\zeta_i - \sum_{j=1}^{N} ca_{ij} DH(s)\zeta_j, \quad i = 1,...,N$$

where $Df(s)$ and $DH(s)$ are the Jacobi matrices of $f(s)$ and $H(s)$ evaluated at s, respectively. Setting $\xi = [\xi_1, ..., \xi_N]$ will transform the above to

$$\dot{\zeta} = Df(s)\zeta - cDH(s)\zeta A^T$$

Furthermore, diagonalize $A^T = S\Lambda S^{-1}$ with a diagonal matrix $\Lambda = diag(\lambda_1, \cdots, \lambda_N)$, where $\{\lambda_k\}_{k=1}^N$ are eigenvalues of matrix A, with $\lambda_1 = 0$. Then, by denoting $\eta = [\eta_1, ..., \eta_N] = \xi S$, one has

$$\dot{\eta} = Df(s)\eta - cDH(s)\eta\Lambda$$

which is equivalent to

$$\dot{\eta}_k = [Df(s)\eta - c\lambda_k DH(s)]\eta_k, \qquad k = 2,..., N \tag{7-9}$$

To this end, a criterion for the synchronization manifold to be (asymptotically) stable is that all the transversal Lyapunov exponents of the variational equation (7-9) are strictly negative [11-14].

Note that in (7-9), each equation has the same form and only η_k and λ_k depend on k. For $k = 1$, the variational equation (not shown in (7-9)) corresponds to the synchronization manifold associated with $\lambda_1 = 0$; for all other $k = 2,..., N$, they correspond to the transversal eigenvectors that span some subspaces, referred to as transversal modes.

Note also that when matrix A is asymmetric (in directed networks, for instance), its eigenvalues can have complex values, so it is natural to replace $c\lambda_k$ by a complex number $(\alpha + i\beta)$ in each equation and then define the following so-called *master stability equation* for all $k = 2,..., N$:

$$\dot{y} = [Df(s) + (\alpha + i\beta)DH(s)]y \tag{7-10}$$

Since this may be a time-varying system, particularly if $s(t)$ is a time function, its eigenvalues may not be useful for determining the stability. Thus, the maximum Lyapunov exponent $L_{\max}$ of the system will be used instead, which is a function of α and β, and is called the *master stability function* [11,13].

For a given and fixed coupling strength c, one can find a point $c\lambda_k$ on the plane (α, β), at which the sign of $L_{\max}$ indicates the stability of the corresponding transversal mode: a negative sign means stability and a positive sign means instability of the transversal mode.

Furthermore, if all transversal modes of λ_k are stable, $k = 2, \ldots, N$, then the synchronization manifold of the original network (7-1) is stable, implying that the network achieves synchronization.

Example 7.1 Consider a network of N Rössler oscillators, in which the i th node is described by

$$\dot{x}_i^{(1)} = -(x_i^{(2)} + x_i^{(3)})$$
$$\dot{x}_i^{(2)} = x_i^{(1)} + a x_i^{(2)}$$
$$\dot{x}_i^{(3)} = b + x_i^{(3)}(x_i^{(1)} - c)$$

When $a = 0.2$, $b = 0.2$, $c = 5.7$, this Rössler oscillator has a chaotic attractor as shown in Fig. 7-1.

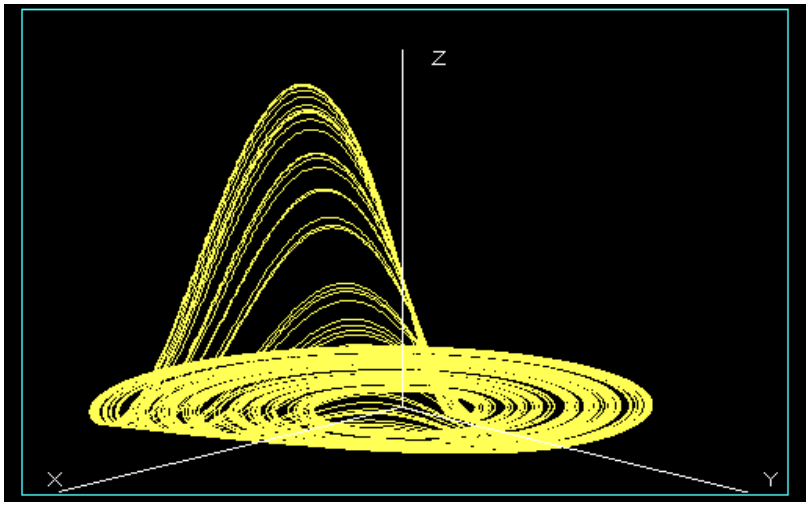

Fig. 7-1 Rössler chaotic attractor

Suppose that all nodes are coupled through the first components $x_i^{(1)}$ of their state vectors, $i = 1,2,...,N$. In this case, the inner coupling function is a 3×3 matrix of the form $diag\{1,00\}$.

The master stability function of this network of Rössler oscillators is shown in Fig. 7-2 [13], where dash curves are negative Lyapunov exponents, solid curves are positive Lyapunov exponents, and black dots are the (α, β) values, of a ring of 10 Rössler oscillators. The inset (a) shows a typical master stability function surface which is basically symmetrical about the α-axis along β. From the inset (a) it can be seen that corresponding to $\alpha = \beta = 0$, i.e., corresponding to the coupling strength $c = 0$ (uncoupled), one has $L_{\max} > 0$, implying that each individual Rössler is chaotic. For fixed $\beta = 0$, as α decreases (i.e., c increases), after a threshold value, $L_{\max}$ will decrease to be negative; as α continues to decrease, however, after another threshold value, $L_{\max}$ will return to be positive again. This example demonstrates that too strong or too weak a coupling strength will lead the synchronization manifold of a coupled network to become unstable, i.e., desynchronized.

For undirected and unweighted networks, the eigenvalues of their outer coupling matrix A are all real, as listed in (7-3) above. In this case, the corresponding master stability equation (7-10) can be simplified to

$$\dot{y} = [Df(s) + \alpha DH(s)]y \tag{7-11}$$

Hence, the corresponding $L_{\max}$ is a function of the real parameter α. The range of α that guarantees $L_{\max}$ be negative is called a *synchronization region*, denoted by S, on which network (7-1) will achieve synchronization. It can be seen that this region is determined by the node dynamics $f(\cdot)$ as well as the inner coupling function $H(\cdot)$.

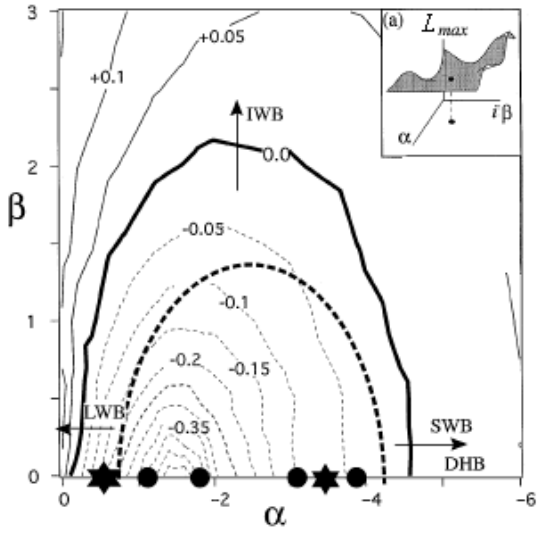

Fig. 7-2 Master stability function of the $x^{(1)}$-coupled Rössler network [13]

Furthermore, if

$$c\lambda_k \subseteq S, \quad k = 2, ..., N \tag{7-12}$$

then the synchronization manifold will be stable. Therefore, according to its different synchronization regions S, network (7-1) is classified into the following types (see Fig. 7-3, [37,42]):

Type-I: Synchronization region is $S_1 = (-\infty, -\alpha_1)$, where α_1 is a finite nonnegative number. For this type of networks, if

$$c\lambda_2 > \alpha_1 \tag{7-13}$$

or

$$c > \frac{\alpha_1}{\lambda_2} > 0 \tag{7-14}$$

then the synchronization manifold of the network is stable. Thus, the synchronizability of Type-I networks is determined by the second eigenvalue λ_2 of its outer coupling matrix A. The smaller the λ_2, the stronger the synchronizability of the network. The inequality (7-13) or (7-14) is the basic criterion for Type-I network synchronizability.

Type-II: Synchronization region is $S_2 = (-\alpha_1, -\alpha_2)$, where α_1 and α_2 are finite nonnegative real numbers, with $\alpha_2 < \alpha_1$. For this type of networks, if

$$\frac{\alpha_1}{\lambda_2} < c < \frac{\alpha_2}{\lambda_N} \tag{7-15}$$

or

$$c > \frac{\alpha_1}{\alpha_2}\frac{\lambda_N}{\lambda_2} > 0 \tag{7-16}$$

then the synchronization manifold of the network is stable. Similarly, inequality (7-15) or (7-16) is referred to as the basic criterion for Type-II network synchronizability which, in case the coupling strength is a variable parameter, can be simply written as

$$0 < \frac{\lambda_N}{\lambda_2} < c \tag{7-17}$$

Thus, the synchronizability of Type-II networks are characterized by the ratio λ_N / λ_2 of the two eigenvalues of the outer coupling matrix A. The smaller the λ_N / λ_2, the stronger the synchronizability of the network.

Type-III: Synchronization region is a union of an interval of the form $(-\infty,-\alpha_1)$ and some regions of the form $(-\alpha_1,-\alpha_2)$, for instance, in the form of $(-\infty,-\alpha_1)\cup(-\alpha_2,-\alpha_3)$ or $(-\alpha_1,-\alpha_2)\cup(-\alpha_3,-\alpha_4)$ or $(-\alpha_1,-\alpha_2)\cup(-\alpha_3,-\alpha_4)\cup(-\alpha_5,-\alpha_6)$, and so on [42].

Type-IV: Synchronization region does not exist, i.e., is an empty set. For this type of networks, any coupling strength and coupling matrix will not be able to lead the network to synchronize.

As mentioned, the synchronization region is determined by the node dynamics $f(\cdot)$ as well as the inner coupling function $H(\cdot)$. For a connected network, if the coupling strength c is large enough, a Type-I network will always synchronize; but only if c is inside a certain value range will a Type-II or Type-III network synchronize.

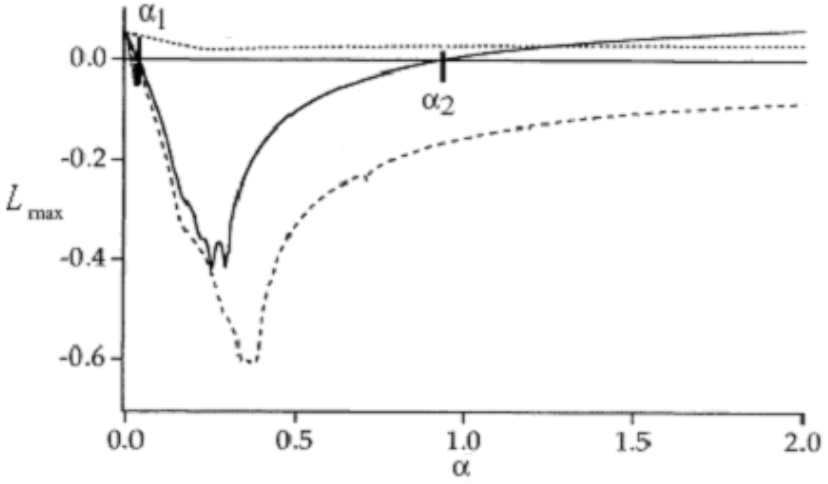

Fig. 7-3 Master stability functions of different types of networks [37]

In applications, to determine the synchronization region of a given network, those thresholds α_1, α_2, …, are usually determined by numerical simulations. Only for some special inner coupling function $H(\cdot)$ may these thresholds be derived via theoretical analysis, as further discussed below.

7.2.2 Complete Synchronization of Linearly Coupled Continuous-Time Networks

When the inner coupling function $H(\cdot)$ is linear, it is simply an $n\times n$ matrix H. In this case, network (7-1) reduces to [15-19]

$$\dot{x}_i = f(x_i) - c\sum_{j=1}^{N} a_{ij} H x_j, \qquad i = 1,...,N \tag{7-18}$$

where typically $H = diag\{r_1, r_2, \cdots, r_n\}$, describing the way of coupling among components of state vectors. For instance, in Example 7.1, $n=3$, $r_1=1$, $r_2=0$ and $r_3=0$.

The following result is a consequence of the above discussion.

Theorem 7-1 [16] *For network* (7-18)*, if the following system of n-dimensional linear time-varying systems*

$$\dot{w} = [Df(s) - c\lambda_k H]w, \qquad k = 2,...,N \tag{7-19}$$

are exponentially stable, then the synchronization manifold of network (7-18) *is also exponentially stable.*

Theorem 7-2 [16] *For network* (7-18)*, if there exist an $n\times n$ diagonal matrix $E>0$ and two constants $\bar{d}<0$ and $\tau>0$, such that for all $d\le\bar{d}$,*

$$[Df(s) - dH]^T E + E[Df(s) - dH] \le -\tau I_n \tag{7-20}$$

where I_n is the identity matrix, and if

$$c\lambda_2 \ge \bar{d} \tag{7-21}$$

then the synchronization manifold of network (7-18) *is exponentially stable.*

Proof. It follows from (7-21) and (7-3) that

$$c\lambda_k \ge \bar{d}, \qquad k = 2,...,N \tag{7-22}$$

Substituting it into (7-20) gives

$$[Df(s) - c\lambda_k H]^T E + E[Df(s) - c\lambda_k H] \le -\tau I_n, \qquad k = 2,...,N$$

Then, by defining Lyapunov functions of the form $V_k = \zeta^T E\zeta$, $k=2,...,N$, one can easily show that system (7-19) is exponentially stable about its zero equilibrium. To this end, Theorem 7-1 implies that the synchronization manifold of network (7-18) is exponentially stable. □

Theorem 7-3 [21] *For a network* (7-18) *with identical chaotic nodes, if the inner coupling matrix H is an identity matrix, and if the maximum Lyapunov exponent $h_{\max}$ of any individual node satisfies*

$$c\lambda_2 \geq h_{\max} \tag{7-23}$$

then the synchronization manifold of network (7-18) *is exponentially stable.*

It is clear from (7-21) and (7-23, or $c \geq \alpha/\lambda_2$ where $\alpha = \bar{d}$ or $\alpha = h_{\max}$, that the larger the λ_2, the smaller the coupling strength c is required to achieved the network synchronization. In other words, larger λ_2 leads to better synchronizability.

7.3 Complete Synchronization of Typical Dynamical Networks

7.3.1 Complete Synchronization of Regular Networks

Type-I Networks

Recall that the synchronizability of Type-I networks is determined by the second eigenvalue λ_2 of the Laplacian matrix $-A$.

A nearest-neighbor coupled network of N nodes with degree K (assumed to be an even integer) has a Laplacian matrix $-A_{nc}$ in the following circulant form:

$$-A_{nc} = -\begin{bmatrix} -K & 1 & \cdots & 1 & 0 & \cdots & 0 \\ 0 & -K & 1 & \cdots & 1 & 0 & 0 \\ 0 & 0 & -K & 1 & \cdots & 1 & 0 \\ \vdots & & & \ddots & & & \vdots \\ 1 & 0 & 0 & \cdots & -K & 1 & 1 \\ 1 & \cdots & 0 & 0 & 0 & -K & 1 \\ 1 & \cdots & 1 & 0 & \cdots & 0 & -K \end{bmatrix}$$

with the second eigenvalue

$$\lambda_{2nc} = 4\sum_{j=1}^{K/2} \sin^2(j\pi/N)$$

Clearly, for any fixed K, $\lambda_{2nc} \to 0$ monotonically as $N \to \infty$, implying that it is difficult for a nearest-neighbor coupled network to achieve synchronization if its size is too large.

A fully coupled network of N nodes has a Laplacian matrix $-A_{gc}$, with

$$A_{gc} = \begin{bmatrix} -N+1 & 1 & \cdots & \cdots & 1 \\ 1 & -N+1 & 1 & \cdots & 1 \\ \vdots & \ddots & \ddots & \ddots & \vdots \\ 1 & \cdots & 1 & \ddots & 1 \\ 1 & \cdots & \cdots & 1 & -N+1 \end{bmatrix}$$

which has a single zero eigenvalue of multiplicity 1 and all the other eigenvalues are equal to $-N$. So, as $N \to \infty$, its second eigenvalue of the corresponding Laplacian

matrix satisfies $\lambda_{2gc} = N \to \infty$ monotonically, implying that a fully coupled network can easily achieve synchronization if its size is large enough.

A star-shaped network of N nodes has a Laplacian matrix $-A_{sc}$, with

$$A_{sc} = \begin{bmatrix} -N+1 & 1 & 1 & \cdots & 1 \\ 1 & -1 & 0 & \cdots & 0 \\ \vdots & \ddots & \ddots & \ddots & \vdots \\ 1 & 0 & 0 & \ddots & 0 \\ 1 & 0 & 0 & \cdots & -1 \end{bmatrix}$$

The corresponding Laplacian matrix has the second eigenvalue $\lambda_{2sc} = 1$, which is independent of the network size. Hence, the synchronizability of a star-shaped network is independent of the network size.

In summary, for Type-I linearly and diffusively coupled networks (7-1):

1. For a fixed coupling strength $c > 0$, no matter how strong it is, when the size of a nearest-neighbor coupled network is large enough, the network is difficult to achieve synchronization.

2. For a fixed coupling strength $c > 0$, no matter how weak it is, when the size of a fully coupled network is large enough, the network will synchronize.

3. For a star-shaped network, the network synchronizability is independent of the network size; namely, when the coupling strength $c > 0$ is larger than a threshold, which is independent of the network size, the network will synchronize.

Type-II Networks

Recall that the synchronizability of Type-II networks is determined by the ratio of the N th and the second eigenvalues, λ_N / λ_2, of the Laplacian matrix $-A$.

A nearest-neighbor coupled network of N nodes with degree K (assumed to be an even integer), the eigenvalues of its Laplacian matrix $-A_{nc}$ satisfy [28]

$$\frac{\lambda_{Nnc}}{\lambda_{2nc}} \approx \frac{(3\pi + 2)N^2}{2\pi^2(K+1)(K+2)} \text{ for } 1 << K << N$$

Therefore, $\lambda_N / \lambda_2 \to \infty$ as $N \to \infty$, implying that the synchronizability of the network is very weak.

A fully coupled network has all nonzero Laplacian eigenvalues $\lambda_2 = \cdots = \lambda_N = N$, so that $\lambda_N / \lambda_2 \equiv 1$. Therefore, as long as the coupling strength $c > 1$, the network will synchronize.

A star-shaped network has $\lambda_N / \lambda_2 \equiv N$, so $\lambda_N / \lambda_2 \to \infty$ as $N \to \infty$, implying that it is generally difficult for the network to achieve synchronization.

In summary, for Type-II linearly and diffusively coupled networks (7-1):

1. For a fixed coupling strength $c > 0$, no matter how strong it is, when the sizes of a nearest-neighbor coupled network and a star-shaped network are large enough, these networks are difficult to achieve synchronization.

2. For a fully coupled network, the network synchronizability is independent of the network size; if the coupling strength $c > 1$, then the network will synchronize.

7.3.2 Synchronization of Small-World Networks

Consider an NW small-world network (7-1) of N dynamical systems. Only Type-I networks are discussed here [15].

Notice that in the NW small-world network model, the process of adding an edge with probability p means that in the outer coupling matrix A, the corresponding 0 element is being replaced by 1 with probability p.

In simulating a nearest-neighbor coupled network, in its outer coupling matrix A_{nc}, one may first replace its zero elements $a_{ij} = a_{ji} = 0$ by $a_{ij} = a_{ji} = 1$ with probability p, then recalculate its diagonal elements by using formula (7-2) to obtain a new outer coupling matrix, hence a new Laplacian matrix $-A_{nw}(p, N)$, and finally calculate its eigenvalues to obtain the second eigenvalue $\lambda_{2nw}(p, N)$.

Simulations on the NW small-world network model of sizes $N = 200$ and $N = 500$, respectively, with different probabilities p, are shown in Fig. 7-4 [12]. It can be seen that for the nearest-neighbor coupled network (with $p = 0$) has $\lambda_{2nm}(p, N) \approx 0$, therefore its synchronizability is very weak. As more new edges are being added to the network (i.e., as p is increased from 0 to 1), one has $\lambda_{2nm}(p, N) \to N$, showing that the synchronizability of the network is increasing. This implies that for any fixed coupling strength $c > 0$, if the network has a large enough number of nodes so that condition (7-21) is satisfied, i.e., $N > \overline{d} / c$, then as the probability p becomes larger than a threshold $\overline{p}$, $\overline{p} \le p \le 1$, the network will synchronize.

Figure 7-5 [15] shows the changes of the second eigenvalue of the outer coupling matrix A_{nw} versus N in an NW small-world network, with $p = 0.05$ and $p = 0.1$, respectively. It can be seen that for the same p, the larger the N, the stronger the synchronizability of the network.

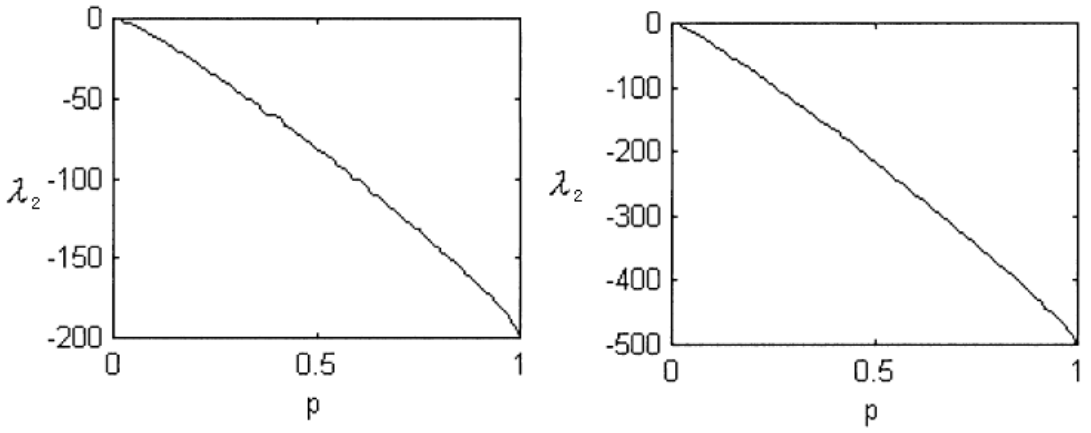

(a) $N = 200$ (b) $N = 500$

Fig. 7-4 Changes of the second eigenvalue of A_{nw} versus p [15]

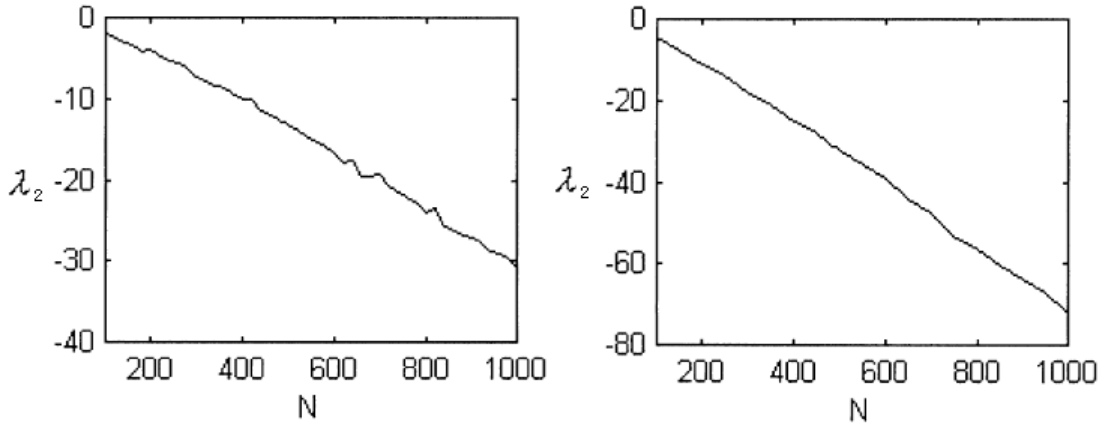

(a) $p = 0.05$ (b) $p = 0.1$

Fig. 7-5 Changes of the second eigenvalue of A_{nw} versus N [15]

7.3.3 Synchronization of Scale-Free Networks

BA Scale-Free Networks

Now, consider a BA scale-free network in the form of (7-1) with N dynamical systems. Only Type-I networks are discussed here [16].

In constructing the BA model, let $m_0 = m = \hat{m}$ and denote its outer coupling matrix by $A_{sf}(\hat{m}, N)$, hence its Laplacian matrix by $-A_{sf}(\hat{m}, N)$ with the second eigenvalue $\lambda_{2sf}(\hat{m}, N)$.

Simulations show that $\lambda_{2sf}(\hat{m}, N)$ increases as N increases, and

$$\lim_{N\to\infty} \lambda_{2sf}(\hat{m}, N) = \hat{\lambda}_{2sf}(\hat{m}) > 0$$

Figure 7-6 [16] shows the changes of $\lambda_2 = -\lambda_{2sf}(\hat{m}, N)$ versus different values of $\hat{m}$ and N : when $m_0 = m = 3,5,7$, $\lambda_2 \approx -1.2,-2.9,-4.6$, respectively. It can be seen that the network synchronizability will saturate, namely, for large enough N , continuously increasing the number of new nodes does not change the network synchronizability significantly.

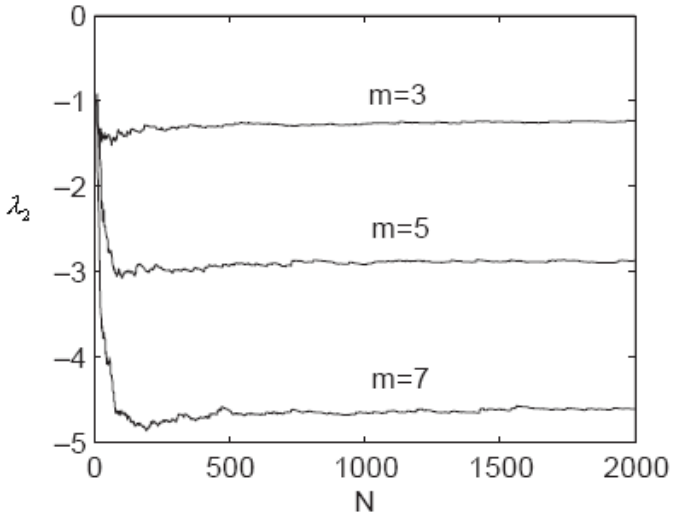

Fig. 7-6 Changes of λ_2 versus N [16]

Synchronization-Optimal Networks

From the above discussions, one can see that a network with a larger number of edges usually has a stronger synchronizability, which is generally true for typical regular networks, random networks, small-world networks, and scale-free networks. A natural question is: if the number of edges is given and fixed, what kind of network has the strongest synchronizability? One possible answer is given by the following so-called synchronization-optimal network model [38]:

1. Start with a small network of $m_0 > 0$ nodes.

2. *Growth*: In each step, add one new node to the network, with m ($m \le m_0$) edges connecting to randomly selected existing nodes.

3. *Optimal Attachment*: The way of a new edge connecting to an existing node is to maximize the synchronizability of the resulting network, i.e., making the second eigenvalue of the resulting network outer coupling matrix as small as possible.

After t steps, the network has $N = t + m_0$ nodes and mt edges, which has the strongest synchronizability as compared to other networks.

Similar to the BA network discussed above, as $N \to \infty$, the second eigenvalue will approach a positive constant value, $\lambda_{2so}(m)$. For example, when $m_0 = m = 3,5,7$, one has $\lambda_{2so}(m) \approx 2.0,4.0,5.9$, respectively. Compared with the BA network model discussed above, however, these three eigenvalues are all much smaller, implying significant improvement of the network synchronizability.

Analysis further shows that the topology of this synchronization-optimal network model is similar to a multi-center network: a few nodes are connected to big nodes (hubs), while the majority of nodes have small degrees. This structural characteristic helps increase the network synchronizability, yet it also makes the network more vulnerable (i.e., less robust) to attacks, leaving an important issue for future studies.

Synchronization-Preferred Network

To balance the stronger synchronizability and robustness against attacks, the following synchronization-preferred network model may be considered [39]:

1. Start with a small network of $m_0 > 0$ nodes.

2. *Growth*: In each step, add one new node to the network, with m ($m \le m_0$) edges connecting to randomly selected existing nodes.

3. *Preferential Attachment*: A new edge is connecting to an existing node i with the following probability:
$$\Pi_i = \lambda_{2i} \Big/ \sum_j \lambda_{2j}$$
where λ_{2i} is the second eigenvalue of the outer coupling matrix of the network when the new node had just been added to node i.

After t steps, the network has $N = t + m_0$ nodes and mt edges, with a preferred synchronizability.

For a fixed m, as $N \to \infty$, the second eigenvalue will approach a negative constant value, $\lambda_{2sp}(m)$. For example, when $m_0 = m = 3,5,7$, one has $\lambda_2 = -\lambda_{2sp}(m) \approx -1.3,-2.9,-4.6$, respectively.

Now, in the case of $m_0 = m = 3$, Fig. 7-7 [39] compares the simulation results on the second eigenvalues of the BA network (solid curve with small circles), synchronization-optimal network (dash curve with diamonds), and synchronization-preferred network (dot-dash curve with small squares).

It is clear that the last two models have about the same synchronizability. However, it will be shown in the next subsection that the synchronization-preferred network model significantly improves the network robustness against attacks.

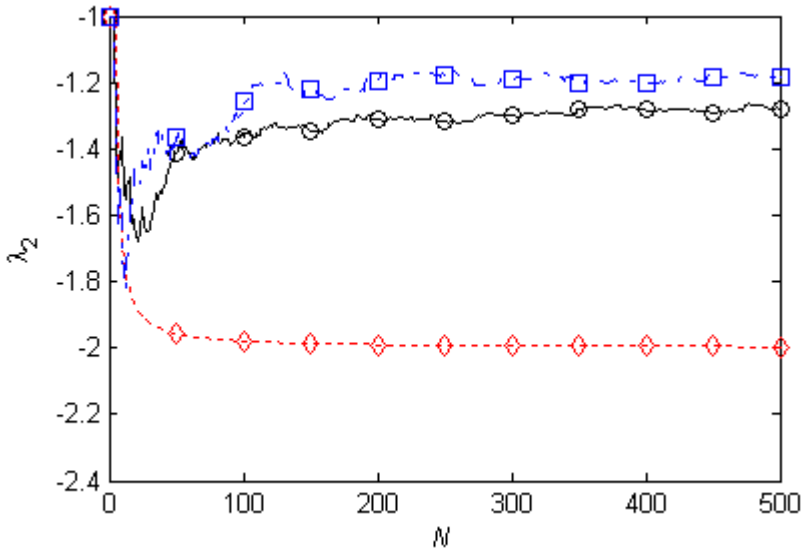

Fig. 7-7 Comparison of synchronizability of three network models [39]

Robustness and Fragility of Scale-Free Networks against Attacks

The robustness and fragility of scale-free networks were analyzed in Section 3.5.2, Chapter 3. This issue is revisited here from a synchronization point of view.

Consider a scale-free network in the form of (7-1), with N nodes and an outer coupling matrix $A_{sf} \in R^{N\times N}$. Suppose that the network is now being attacked, so a small fraction f of nodes have been destroyed therefore removed, where $0 < f < 1$. Let the removed nodes be denoted by $i_1, i_2, \cdots, i_{[fN]}$, where $[fN]$ is the integer part of real number fN. Accordingly, the elements of A_{sf} on the $i_1, i_2, \cdots, i_{[fN]}$ rows and the $i_1, i_2, \cdots, i_{[fN]}$ columns become zero, so A_{sf} reduces to $\overline{A}_{sf}$. Consequently, the diagonal elements of $\overline{A}_{sf} = [\overline{a}_{ij}]$ also need to be recalculated, by formula (7-2), resulting in a new outer coupling matrix, $\tilde{A}_{sf} = [\tilde{a}_{ij}]$. To this end, let λ_{2sf} and $\tilde{\lambda}_{2sf}$ be the second eigenvalues of Laplacian matrices A_{sf} and $\tilde{A}_{sf}$, and denote $\lambda_2 = -\lambda_{2sf}$ and $\tilde{\lambda}_2 = -\tilde{\lambda}_{2sf}$, respectively.

In the case of random attacks or random failures, due to the heterogeneity of the scale-free networks, the nodes being removed are generally small-degree nodes; therefore, $\lambda_{2sf} \approx \tilde{\lambda}_{2sf}$, so the synchronizability of the resulting network will remain basically unchanged. A simulation on a BA scale-free network with $N = 2000$ and $m_0 = m = 3$ shows that after 5% of nodes have been removed, the network remains being connected, with $\tilde{\lambda}_2 < -0.5$, as seen in Fig. 7-8 [39]. In this figure, four different types of networks are compared: the random-graph network (solid curve with small stars), the BA network

(solid curve with small circles), the synchronization-optimal network (dash curve with diamonds), and the synchronization-preferred network (dot-dash curve with small squares).

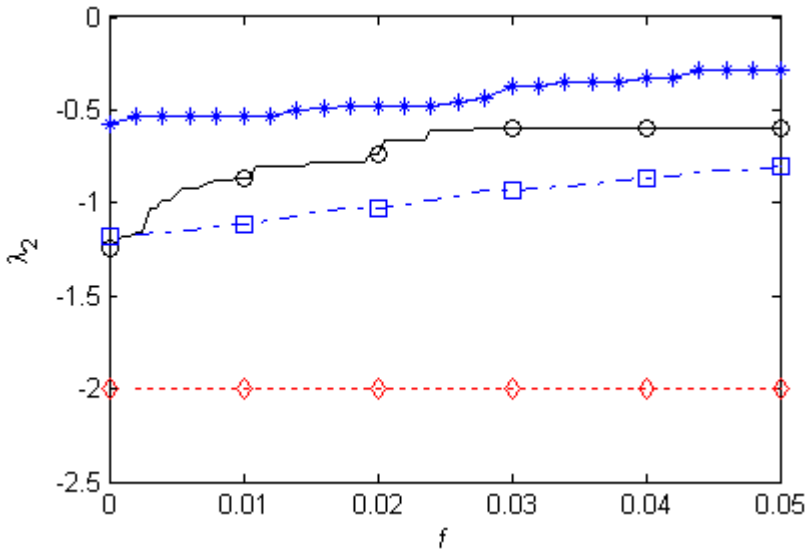

Fig. 7-8 Comparison of synchronization robustness for four types of networks [39]

It can be seen from Fig. 7-9 [39], where $\lambda_{2LC} = \lambda_2$ here, that under an intentional attack to a scale-free network, some largest-degree nodes were removed, so the network topology had a drastic change and even became unconnected, which results in $\lambda_{2sf} >> \tilde{\lambda}_{2sf}$. Consequently, the synchronizability of the network is significantly reduced. In the simulation, even only 0.7% of hub nodes (largest-degree ones) were removed, the network became unconnected, leading to $\tilde{\lambda}_{2BA} = 0$, as shown by the dash curve in the figure. The inset in Fig. 7-9 shows the percentage of the remaining connected sub-nets in the whole network after a fraction f of nodes (the horizontal axis) had been removed. It can be seen that if 5% of largest-degree nodes were removed, even in the largest connected sub-net, its synchronizability had a significant decrease. It is notable that for synchronization-optimal networks, since it has a multi-center structure, it is more vulnerable to intentional attacks: after as less as m_0 largest-degree nodes were removed, the whole network was broken to be a set of isolated nodes. But, on the other hand, since the majorities of nodes in this kind of networks are small-degree nodes, they are very robust against random attacks.

7.3.4 Complete Synchronization of Local-World Networks

Consider the so-called Local-World (LW) model, a special case of the Multi-Local World (MLW) model studied in Section 3.5.4, Chapter 3.

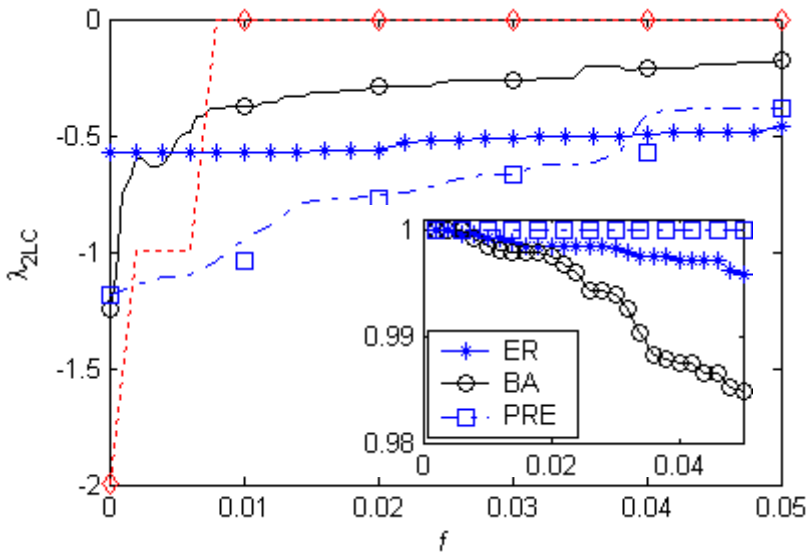

Fig. 7-9 Comparison of synchronization fragility for four types of networks [39]

The LW network model is essentially heterogeneous, with a degree distribution in between the exponential distribution and the power-law distribution. Therefore, LW networks generally have robustness and fragility also in between exponential networks and scale-free networks, as shown by Figs. 7-10 and 7-11 [22].

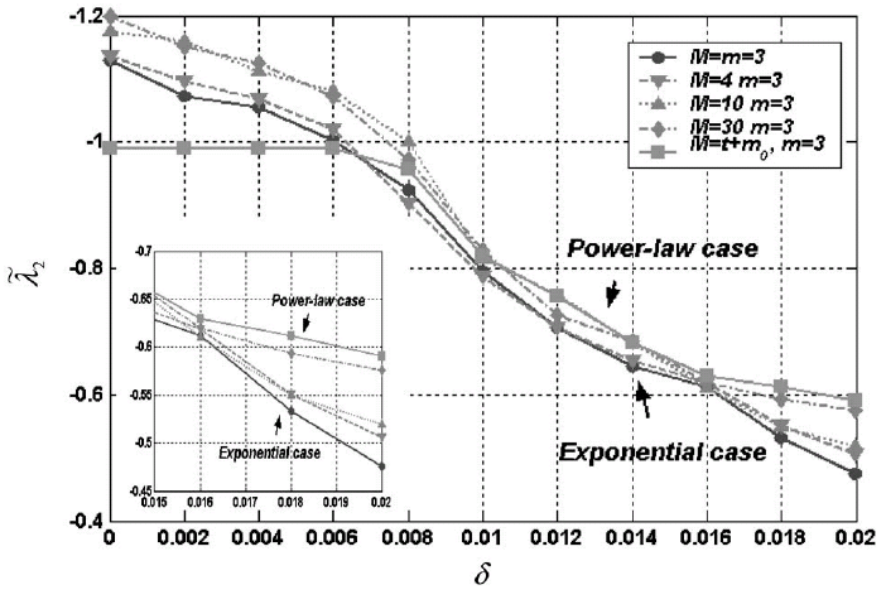

Fig. 7-10 Comparison of synchronization robustness [22]
(Inset is an enlargement of segment $0.015 \le \delta \le 0.02$)

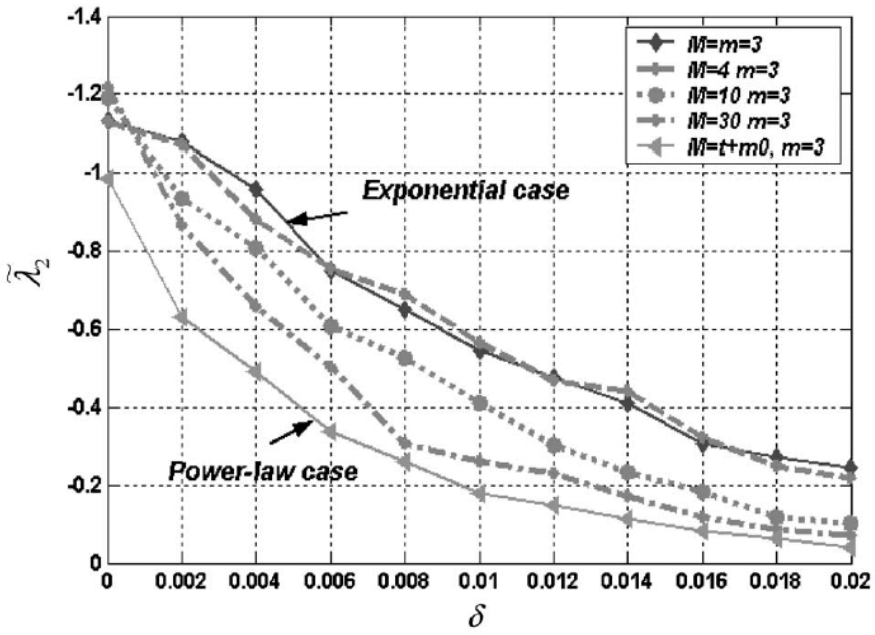

Fig. 7-11 Comparison of synchronization fragility [22]

7.4 Phase Synchronization

Consider two coupled dynamical systems with oscillatory behaviors, referred to as oscillators, where the oscillations are completely characterized by their amplitudes and phases.

Definition 7.2 If the phases ϕ_1 and ϕ_2 of two coupled oscillators has a certain ratio $n:m$, where n and m are integers, ideally $|n\phi_1 - m\phi_2| = 0$ or practically $|n\phi_1 - m\phi_2| \le \varepsilon$ (a small constant), then these two oscillators are said to achieve (ideal or practical) *phase synchronization*.

Clearly, phase synchronization is a kind of weak synchronization, since when phase synchronization is achieved, the phases of the oscillators are locked but their amplitudes may be different.

7.4.1 Phase Synchronization of the Kuramoto Model

In the studies of phase synchronization, the Kuramoto model is a common platform [6,43,44]:

$$\dot{\theta}_i = \omega_i + \sum_{j=1}^{N} \Gamma_{ij}(\theta_j - \theta_i), \qquad i = 1,\ldots,N \tag{7-24}$$

Here, θ_i and ω_i are the phase and natural frequency of oscillator i, $i = 1,2,...,N$, respectively, in which all ω_i have the same probability distribution $g(\omega)$. For simplicity, assume that $g(\omega)$ is a symmetric function with a single peak, such as Gaussian,

satisfying $g(\omega) = g(-\omega)$, and $g(\omega)$ is non-increasing on interval $[0, \infty)$. Moreover, for fully coupled equally-weighted networks, consider the simple case

$$\Gamma_{ij}(\theta_j - \theta_i) = \frac{c}{N}\sin(\theta_j - \theta_i)$$

where $c \geq 0$ is a constant coupling strength. In this case, (7-24) can be rewritten as

$$\dot{\theta}_i = \omega_i + \frac{c}{N}\sum_{j=1}^{N}\sin(\theta_j - \theta_i) \tag{7-25}$$

To better understand the dynamical behaviors of the phases during the process of synchronization, imagine a group of nodes moving along a circular path, as illustrated by Fig. 7-12. Introduce an *order parameter* defined by

$$re^{i\psi} = \frac{1}{N}\sum_{j=1}^{N} e^{i\theta_j} \tag{7-26}$$

in which $r = r(t)$ measures the coherence of the group of moving nodes and $\psi = \psi(t)$ represents their average phase. Here, r can be used to describe the ratio of the number of the synchronous nodes over the total number of nodes, as illustrated by Fig. 7-12.

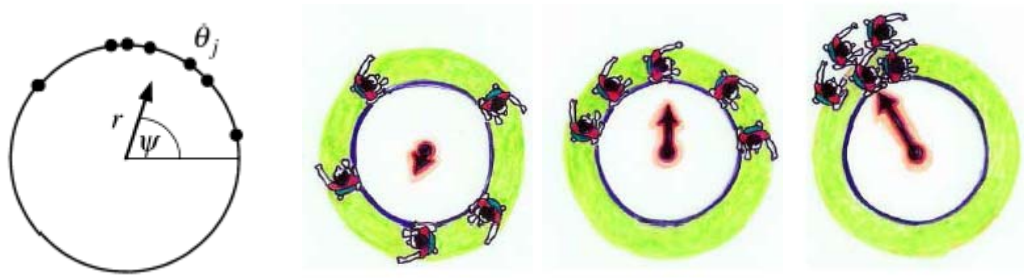

(a) order parameter (b) $r \approx 0$ (c) $0 << r << 1$ (d) $r \approx 1$

Fig. 7-12 Geometric meaning of the order parameter

Using the order parameter, (7-25) can be rewritten as

$$\dot{\theta}_i = \omega_i + Kr\sin(\psi - \theta_i), \quad i = 1,2,...,N \tag{7-27}$$

which has a mean-field characteristic, with an effective coupling strength Kr. When synchronized, all $\theta_i \to \psi$ as $t \to \infty$, $i = 1,2,...,N$.

Now, assume that $g(\omega)$ is Gaussian. Figure 7-13 [44] shows that when $K < K_c$, a threshold, all nodes will oscillate according to their individual natural frequencies, independent of their initial phases, in a way just like they are uncoupled. Moreover, $r(t)$ decreases exponentially fast, to be about $O(N^{-1/2})$. The figure also shows that when $K > K_c$, $r(t)$ increases exponentially fast, implying that a sub-group of the nodes start to synchronize, till a saturated value of $r_\infty \approx 1$, when finally all nodes are synchronized.

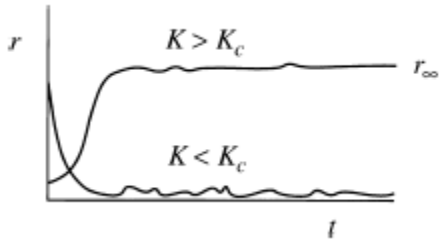

Fig. 7-13 Evolution of $r(t)$ in the Kuramoto model [44]

Next, without loss of generality, assume $\psi \equiv 0$. Then, (7-27) becomes

$$\dot{\theta}_i = \omega_i - Kr\sin\theta_i, \quad i = 1,2,...,N \tag{7-28}$$

For this coupled network, the threshold K_c can be more precisely characterized, as explained below.

The group of nodes can be classified into two sub-groups according to the relative values of $|\omega_i|$ and Kr: for the nodes with $|\omega_i| \le Kr$, since $\dot{\theta}_i \approx 0$, their natural frequencies will be "phase-locked":

$$\omega_i = Kr\sin\theta_i, \quad i = 1,2,...,N \tag{7-29}$$

For those nodes with $|\omega_i| > Kr$, however, they will be "phase-drifted" in an uneven manner.

Now, let $\rho(\theta,\omega)d\theta$ be the portion of nodes with natural frequencies ω in the interval $[\theta,\theta+d\theta]$:

$$\rho(\theta,\omega) = \frac{C}{|\omega - Kr\sin\theta|}$$

where $C = \sqrt{\omega^2 - (Kr)^2}/(2\pi)$, which normalizes $\int_{-\pi}^{\pi}\rho(\theta,\omega)d\theta = 1$.

Since all nodes are classified into two groups, by assuming $\psi \equiv 0$ and setting

$$\left\langle e^{i\theta}\right\rangle = \left\langle e^{i\theta}\right\rangle_{lock} + \left\langle e^{i\theta}\right\rangle_{drift}$$

where $\langle\cdot\rangle$ means taking an average, one has $\left\langle e^{i\theta}\right\rangle = re^{i\psi} = r$, which gives

$$r = \left\langle e^{i\theta}\right\rangle_{lock} + \left\langle e^{i\theta}\right\rangle_{drift}$$

For the phase-locked group, all nodes with $|\omega| \le Kr$ satisfy $\sin\theta = \omega/(Kr)$. Moreover, since $g(\omega) = g(-\omega)$, all locked phases are symmetrically distributed around $\theta = 0$, so that $\left\langle\sin\theta\right\rangle_{lock} = 0$ and

$$\left\langle e^{i\theta}\right\rangle_{lock} = \left\langle\cos\theta\right\rangle_{lock} = \int_{-Kr}^{Kr}\cos\theta(\omega)g(\omega)d\omega$$

It then follows from (7-29) that

$$\left\langle e^{i\theta}\right\rangle_{lock} = \int_{-\pi/2}^{\pi/2} \cos\theta g(Kr\sin\theta) Kr\cos\theta d\theta = Kr\int_{-\pi/2}^{\pi/2} \cos^2\theta g(Kr\sin\theta) d\theta$$

For the phase-drifted group, $\left\langle e^{i\theta}\right\rangle_{drift}$ decays, so

$$r = Kr\int_{-\pi/2}^{\pi/2} \cos^2\theta g(Kr\sin\theta) d\theta$$

It is clear that this equation has a zero solution $r = 0$ for any K, which corresponds to a completely incoherent motion. For any θ and ω, $\rho(\theta,\omega) = 1/2\pi$. A non-zero solution is given by

$$1 = c\int_{-\pi/2}^{\pi/2} \cos^2\theta g(cr\sin\theta) d\theta$$

which corresponds to the synchronization of parts of the nodes. It follows that the synchronization threshold is given by

$$K_c = \frac{2}{\pi g(0)} \tag{7-30}$$

and the order parameter is given by

$$r \approx \sqrt{\frac{16}{\pi K_c^3}\sqrt{\frac{\mu}{-g''(0)}}} \tag{7-31}$$

where $\mu = (K - K_c)/K_c$.

7.4.2 Phase Synchronization of Small-World Networks

Consider a small-world network of coupled oscillators [45]:

$$\dot{\theta}_i = \omega_i + c\sum_{j\in\Lambda_i} \mathbf{sin}(\theta_j - \theta_i), \quad i = 1,2,...,N \tag{7-32}$$

where Λ_i is the neighboring set of node i, and phases θ_i and natural frequencies ω_i have zero-mean uniform distributed initial conditions on $(-1/2,1/2)$ and $\mathbf{(-\pi,\pi)}$, respectively. Similarly, define the average order parameter by

$$r = \left[\left\langle \frac{1}{N}\sum_{j=1}^{N} \mathbf{sin}(\theta_j - \theta_i)\right\rangle\right] \tag{7-33}$$

where $\langle\cdot\rangle$ and $[\cdot]$ represent time average and frequency average, respectively.

Different small-world models generated by different coupling strengths c generally have different phase synchronization characteristics. Figure 7-14 [45] shows the relationship of r versus c for different small-world networks. It can be seen that when the coupling strength is weak, $c \to 0$, all nodes are uniformly distributed in the interval $[0, 2\pi]$, so $r = O\left(1/\sqrt{N}\right)$. This corresponds to the uniform distribution shown in Fig. 7-12 (b), for which no synchronous group exists. As c increases, synchronous group is formed and then grows. As $c \to \infty$, one has $r = 1$, implying that the whole group of nodes synchronize in phase, regardless of the network topology.

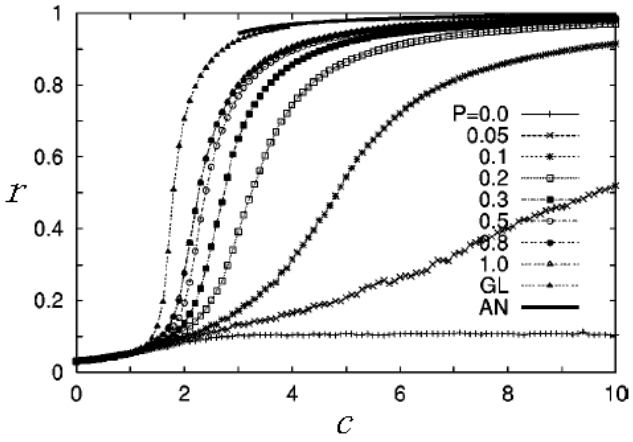

Fig. 7-14 Relationship of r versus c for different small-world networks [45]

It can also be seen from Fig. 7-14 that phase synchronization in a small-world network depends on the edge-addition probability p: when $p = 0$, no long-range edges are added, so no synchronization occurs; as p increases, even for a very small $p = 0.05$, synchronous group emerges and then grows, thereby global synchronization takes place gradually. On the other hand, it is quite interesting to see that for $p > 0.5$, phase synchronization saturates, indicating that a small-world network and a fully connected network behave similarly in phase synchronization. This once again demonstrates the advantage of having a small-world topology for achieving (phase) synchronization, since a small-word network has very few long-range edges as compared to a fully connected network.

7.4.3 Phase Synchronization of Scale-Free Networks

Consider a BA scale-free network of N oscillators, with degree distribution $P(k) \sim k^{-3}$, described also by (7-32), namely [46]

$$\dot{\theta}_i = \omega_i + c \sum_{j \in \Lambda_i} \mathbf{sin}(\theta_j - \theta_i), \; i = 1,2,...,N \tag{7-34}$$

where Λ_i is the neighboring set of node i, and phases θ_i and natural frequencies ω_i have zero-mean uniform distributed initial conditions on $(-1/2,1/2)$ and $\mathbf{(}-\pi,\pi\mathbf{)}$, respectively. Similarly, define the average order parameter by

$$r = \left[\left\langle \frac{1}{N} \sum_{j=1}^{N} \mathbf{sin}(\theta_j - \theta_i) \right\rangle \right] \tag{7-35}$$

where $\langle \cdot \rangle$ and $[\cdot]$ represent time average and frequency average, respectively.

For this scale-free network model, when the coupling strength $c \to 0$, all nodes are oscillating according to their own natural frequencies. As c increases, synchronous group is formed and then grows. After c passes a threshold, the whole network of nodes synchronize in phase. For various BA networks of different sizes (determined by the number m of added new edges), their phase synchronization behaviors are similar, as

shown in Fig. 7-15 [46], where $N = 10{,}000$ and $\lambda = c$.

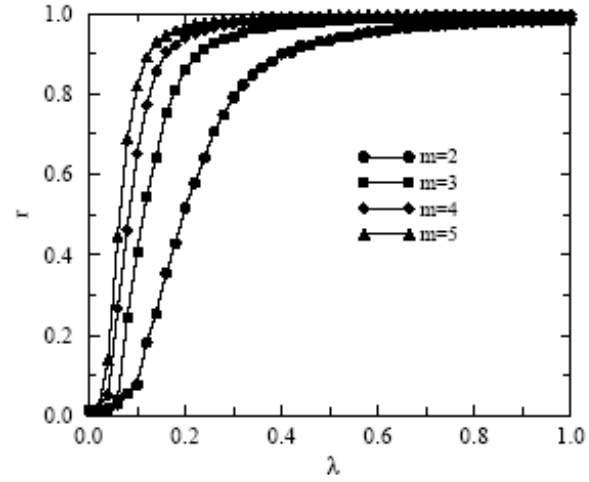

(a) different m

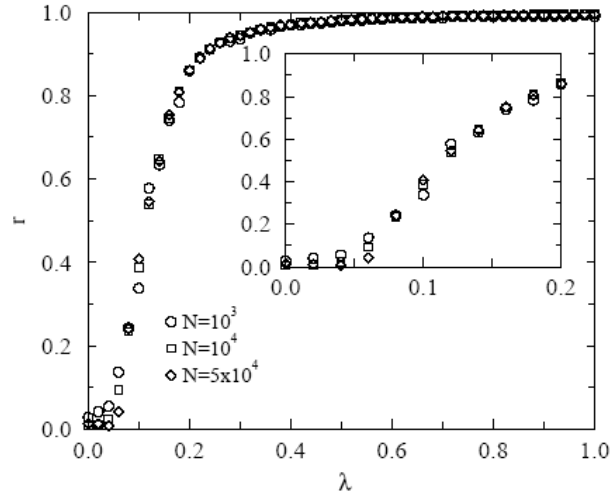

(b) $m = 3$

Fig. 7-15 Relationship of r versus c for different small-world networks [46]

Due to the different heterogeneities of degree distributions in these scale-free networks, their robustness against perturbations are varied. When a scale-free network is slightly perturbed, it may lose global synchrony for some time but then resynchronize again. Figure 7-16 [46] shows the average time $\langle \tau \rangle$ needed for a perturbed network to resynchronize. It can be seen that the data fall into a power-law curve with $\langle \tau \rangle \sim k^{-0.96}$. This means that the bigger the degree of a node, the more stable of the node. It is interesting to see that the instability of a big node (hub) does not affect much on its synchronous group; instead, the neighbors of this hub "help" it re-stabilize itself.

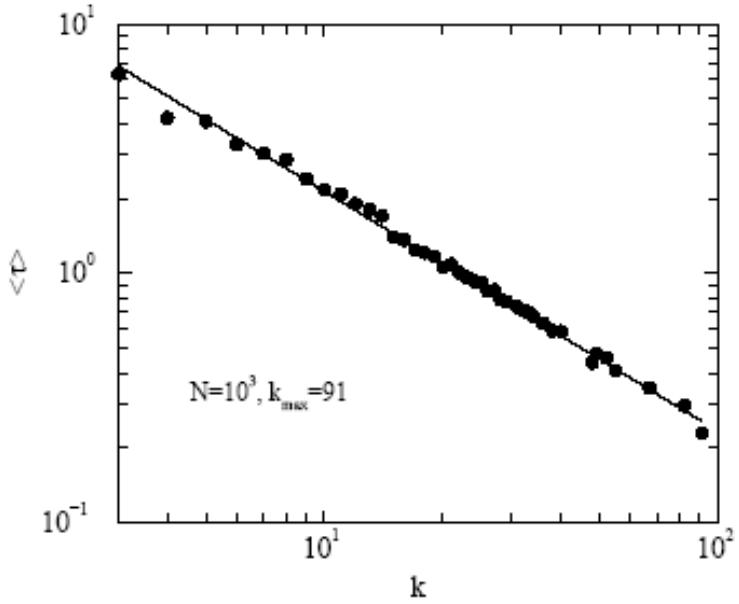

Fig. 7-16 Time needed to resynchronize a perturbed scale-free network [46]

For a scale-free network having a node-degree distribution $k^{-\gamma}$ with $2<\gamma\le 3$, its phase synchronization can be carried out analytically with some approximations [47].

Consider again network (7-34), and let $P(k)$ denote the node-degree distribution and $\rho(k,\omega,t,\theta)$ be the density of nodes with phase θ at time t. Assume, moreover, the normalization condition $\int_0^{2\pi}\rho(k,\omega,t,\theta)d\theta=1$.

When all nodes synchronize, $d\rho/dt=0$, and the evolution of ρ is determined by $\partial\rho/\partial t=-\partial(\rho\upsilon)/\partial\theta$, where υ is a constant. Since the probability of randomly selecting a node with degree k, frequency ω and phase θ is

$$kP(k)N(\omega)\rho(k,\omega,t,\theta)/\int dkkP(k)$$

the density $\rho(k,\omega,t,\theta)$ must satisfy

$$\frac{\partial\rho(k,\omega,t,\theta)}{\partial t}$$
$$=-\frac{\partial}{\partial\theta}\left[\rho(k,\omega,t,\theta)(\omega+\frac{ck\int d\omega'\int dk'\int d\theta' g(\omega')P(k')k'\rho(k',\omega',t,\theta')\sin(\theta'-\theta)}{\int dk'P(k')k'}\right]$$

where, as before, $g(\omega_i)$ is the probability distribution of frequency ω_i, $i=1,2,...,N$.

Defining the order parameter

$$re^{i\psi}=\frac{\int d\omega\int dk\int d\theta g(\omega)P(k)k\rho(k,\omega,t,\theta)e^{i\theta}}{\int dkP(k)k}$$

and substituting it into the above gives

$$\frac{\partial\rho(k,\omega,t,\theta)}{\partial t} = -\frac{\partial(\rho(k,\omega,t,\theta)(\omega + ckr\sin(\psi-\theta)))}{\partial\theta}$$

It then follows from $d\rho/dt = 0$ that

$$\frac{\partial(\rho(k,\omega,t,\theta)(\omega + ckr\sin(\psi-\theta)))}{\partial\theta} = 0$$

Now, without loss of generality, assume that $\psi \equiv 0$. In order to have the same conclusion as the case of a fully coupled network of Kuramoto oscillators studied before, assume that a solution of the above equation is

$$\rho = \begin{cases} \delta(\theta - \arcsin(\omega/ckr)) & if \ \ |\omega/ckr| \le 1 \\ \dfrac{C(k,\omega)}{|\omega - ckr\sin\theta|} & otherwise \end{cases}$$

where $C(k,\omega)$ is a normalized constant. It then follows that

$$r = \frac{\int d\omega\int dk\int d\theta g(\omega)P(k)k\rho(k,\omega;\theta)e^{i\theta}}{\int dkP(k)k} = \frac{cr\int dkk^2P(k)\int_{-1}^{1} d\omega' g(ckr\omega')\sqrt{1-\omega'^2}}{\int dkP(k)k} \quad (7\text{-}36)$$

If $r \neq 0$, then

$$\int dkP(k)k = c\int dkk^2P(k)\int_{-1}^{1} d\omega g(ckr\omega)\sqrt{1-\omega^2}$$

It can be seen that the left-hand side is independent of r. However, the right-hand side depends on r, which is denoted as $f(r)$. When $r = 1$, one has

$$\begin{aligned} \int dkk^2P(k)\int_{-1}^{1} d\omega g(ckr\omega)\sqrt{1-\omega^2} &\le \int dkk^2P(k)\int_{-1}^{1} d\omega g(ckr\omega) \\ &\le \int dk\frac{1}{ckr}k^2P(k)\int_{-\infty}^{\infty} d\omega'' g(\omega'') \\ &= \frac{1}{cr}\int dkkP(k) \end{aligned}$$

Thus, $f(r) \le \int dkkP(k)$. Consequently, for $0 < r \le 1$, equation (7-36) has a solution only if $r = 0$ implies $f(r) > \int dkkP(k)$, namely,

$$\frac{cg(0)\pi\int dkk^2P(k)}{2\int dkP(k)k} > 1 \quad (7\text{-}37)$$

This is a sufficient condition for the network to achieve phase synchronization.

If $P(k) \sim k^{-\gamma}$, with $2 < \gamma \le 3$, then

$$\frac{\int dkk^2P(k)}{\int dkP(k)k} >> 1$$

implying that hubs are very robust against perturbations.

Therefore, for any coupling strength $c > 0$, condition (7-37) is always satisfied, so the threshold for such a scale-free network is almost zero. This is similar to the virus

spreading process on an SIS model, where for a BA scale-free network the epidemic threshold is zero (see Section 5.2.4, Chapter 5).

7.4.4 Phase Synchronization of Non-Uniformly Coupled Networks

In all the network models discussed above, every edge has the same coupling strength. In this subsection, one type of non-uniformly coupled network model is discussed [40]:

$$\dot{\theta}_i = \omega_i + \frac{c}{k_i}\sum_{j=1}^{N} a_{ij}\,\mathbf{sin(}\theta_j - \theta_i\mathbf{)} \tag{7-38}$$

where the coupling strength $c>0$ is a constant; k_i is the degree of node i with a distribution $P(k)$; ω_i is the natural frequency with a distribution $g\mathbf{(}\omega\mathbf{)}$ as before, satisfying $g\mathbf{(}\omega\mathbf{)} = g\mathbf{(}-\omega\mathbf{)}$; $a_{ij}=1$ if node i and node j are connected, $a_{ij}=0$ otherwise, $i, j, = 1,2,...,N$. Clearly, if all $a_{ij}=N$, the network becomes a fully connected network and the model reduces to the standard Kuramoto model discussed before.

Define an order parameter

$$re^{i\psi} = \frac{\int d\omega \int dk \int d\theta g(\omega)P(k)k\rho(k,\omega,t,\theta)e^{i\theta}}{\int dkP(k)k}$$

Then,

$$\frac{\partial\rho(k,\omega,t,\theta)}{\partial t} = -\frac{\partial}{\partial\theta}\left[\rho(k,\omega,t,\theta)\left(\omega + \frac{c}{k}\frac{k\int d\omega'\int dk'\int d\theta' g(\theta')P(k')\rho(k',\omega',t,\theta')\sin(\theta'-\theta)}{\int dk'P(k')k'}\right)\right]$$

$$= -\frac{\partial}{\partial\theta}\left[\rho(k,\omega,t,\theta)\left[\omega + cr\sin(\psi-\theta)\right]\right]$$

In order for $\rho(k,\omega,t,\theta)$ to be a constant, let

$$\rho = \begin{cases} \delta(\theta - \arcsin(\omega/ckr)) & if\ \ |\omega/ckr| \le 1 \\ \dfrac{C(k,\omega)}{|\omega - ckr\sin\theta|} & otherwise \end{cases}$$

where $C(k,\omega)$ is a normalized constant. It then follows that

$$r = cr\int_{-\pi/2}^{\pi/2} d\theta\cos^2\theta g(cr\sin\theta)$$

which eventually gives the following threshold, consistent with (7-30):

$$c^* = \frac{2}{\pi g(0)} \tag{7-39}$$

This means that the threshold of phase synchronization is independent of the coupling strength, verifying once again that a weakly coupled oscillator network may have strong tendency towards synchronization.

Similarly, introduce the average order parameter:

$$r_{av} = \left\langle \left[\frac{\sum_{i=1}^{N} k_i e^{i\theta_i}}{\sum_{i=1}^{N} k_i} \right] \right\rangle$$

where $\langle \cdot \rangle$ and $[\cdot]$ represent time average and frequency average, respectively.

In the following simulation, r_{av} is the average of 10 groups of networks with the same node-degree distribution $P(k)$, where each network takes the average of 5 times of simulations based on the same probability distribution $g(\omega)$, where

$$g(\omega) = \begin{cases} 0.5 & if \quad -1 < \omega < 1 \\ 0 & otherwise \end{cases}$$

It follows from (7-39) that $c^* \approx 1.273$.

Figures 7-17 and 7-18 [40] compare the phase synchronizations of ER random-graph network (dash curve with small circles), BA scale-free network with $P(k) \sim k^{-\gamma}, \gamma = 6$ (solid curves with small diamonds), modified scale-free model (GKK model) [48] (dot-dash curve with small triangles), and local-world (LW) model (dot-dash curves with small squares). All networks have the same size $N = 2048$ and average node-degree $\langle k \rangle = 6$. It can be seen that all network phase synchronization thresholds match (7-39). When $c > c^*$, the average order parameter r_{av} and average value $r_{av} N^{0.25}$ both increase prominently, showing that phase synchronizability is independent of the network topology.

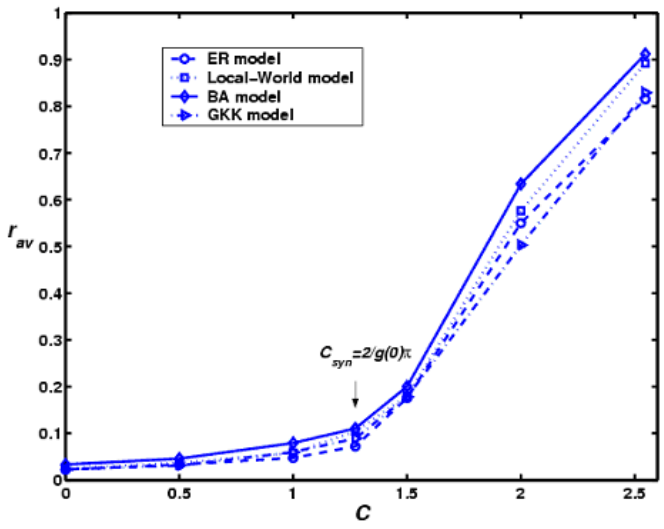

Fig. 7-17 Comparison of average order parameter of four network models [40]

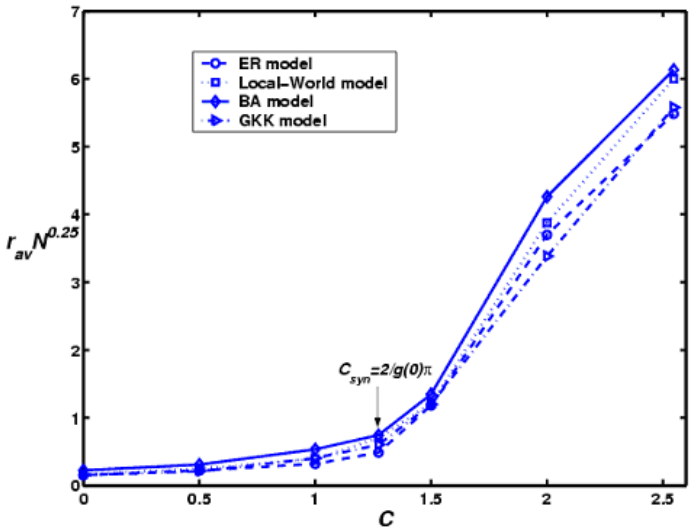

Fig. 7-18 Comparison of average value $r_{av}N^{0.25}$ of four network models [40]

References

[1] Neda Z, Ravasz E, Brechet Y, Vicsek T, Barabasi A-L. The sound of many hands clapping. *Nature*, 2000, 403: 849-850

[2] Blekhman I I. *Synchronization in Science and Technology*. ASME Press, 1988

[3] Strogatz S H. *Sync: The Emerging Science of Spontaneous Order*. New York: Hyperion, 2003

[4] Floyd S, Jacobson V. The synchronization of periodic routing messages. ACM SIGCOMM Computer Communication Review, 1993, 23: 33-44

[5] Winfree A T. Biological rhythms and the behavior of populations of coupled oscillators. *J. Theo. Biol*., 1967, 16: 15-42

[6] Kuramoto Y. *Chemical Oscillations, Waves and Turbulence*. Springer-Verlag, 1984

[7] Kaneko K. *Coupled Map Lattices*. Singapore: World Scientific, 1992

[8] Chua L O. *CNN: A Paradigm for Complexity*. Singapore: World Scientific, 1993

[9] Wu C W, Chua L O. Synchronization in an array of linearly coupled dynamical systems. *IEEE Trans. Circ. Sys.–I*, 1995, 42: 430-447

[10] Wu C W, Chua L O. Application of graph theory to the synchronization in an array of coupled nonlinear oscillators. *IEEE Trans. Circ. Sys.–I*, 1995, 42: 494–497.

[11] Heagy J F, Carroll T L, Pecora L M. Synchronous chaos in coupled oscillator systems. *Phys. Rev. E*, 1994, 50(3): 1874-1885

[12] Ding M Z, Yang W M. Stability of synchronous chaos and on-off intermittency in coupled map lattices. *Phys. Rev. E*, 1997, 56(4): 4009-4016

[13] Pecora L M, Carroll T L. Master stability functions for synchronized coupled systems. *Phys. Rev. Lett*, 1998, 80: 2109

[14] Rangarajan G, Ding M Z. Stability of synchronized chaos in coupled dynamical systems. *Phys. Lett. A*, 2002, 296: 204-209

[15] Wang X F, Chen G. Synchronization in small-world dynamical networks. *Int. J. Bifur. Chaos*, 2002, 12(1): 187-192

[16] Wang X F, Chen G. Synchronization in scale-free dynamical networks: robustness and fragility. *IEEE Trans. Circ. Sys.–I*, 2002, 49(1): 54-62

[17] Wang X F. Complex networks: topology, dynamics and synchronization. *Int. J. Bifur. Chaos*, 2002, 12(5): 885-916

[18] Wang X F, Chen G. Complex networks: small-world, scale-free and beyond, *IEEE Circuits & Systems Magazine*, 2003, 3: 6-20

[19] Wang X F, Chen G. Synchronization in complex dynamical networks, *J. Systems Science and Complexity*, 2003, 16: 1-14

[20] Li X, Wang X F, Chen G. Synchronization in complex dynamical networks and its applications, *Conference on Growing Networks and Graphs in Statistical Physics, Finance, Biology and Social Systems*, Rome, Italy, 2003

[21] Li X, Chen G. Synchronization and desynchronization of complex dynamical networks: an engineering viewpoint. *IEEE Trans. Circuits & Systems-I*, 2003, 50(11): 1381-1390

[22] Li X, Chen G. A local-world evolving network model. *Physica A*, 2003, 328: 274-286

[23] Li X, Jin Y Y, Chen G. Complexity and synchronization of the world trade web. *Phyisca A*, 2003, 328: 287-296

[24] Nishikawa T, Motter A E, Lai Y-C et al. Heterogeneity in oscillator networks: are smaller worlds easier to synchroize? *Phys. Rev. Lett.*, 2003, 91: 014101
[25] Wu C W. Perturbation of coupling matrices and its effect on the synchronizability in arrays of coupled chaotic systems. *Phys. Lett. A*, 2003, 319: 495-503
[26] Hong H, Kim B J, Choi M Y et al. Factors that predict better synchronizability on complex networks. *Phys. Rev. E*, 2004, 69: 067105
[27] Atay F M, Jost J. Delays, connection topology, and synchronization of coupled chaotic maps. *Phys. Rev. Lett.*, 2004, 92: 144101
[28] Barahona M, Pecora L M. Synchronization in small-world systems. *Phys. Rev. Lett*, 2004, 89(5): 054101
[29] Li C, Chen G. Phase synchronization in small-world networks of chaotic oscillators. *Physica A*, 2004, 341: 73-79
[30] Li C, Chen G. Synchronization in general complex dynamical networks with coupling delays. *Physica A*, 2004, 343: 236-278
[31] Lu J, Yu X, Chen G, Cheng D. Characterizing the synchronizability of small-world dynamical networks. *IEEE Trans. Circ. Sys.-I*, 2004, 51: 787-796
[32] Lu J, Chen G. A time-varying complex dynamical network model and its controlled synchronization criteria. *IEEE Trans. Auto. Control*, 2005,50:841-846
[33] Lu J, Yu X, Chen G. Chaos synchronization of general complex dynamical networks. *Physica A*, 2004, 334: 281-302
[34] Motter A E, Zhou C, Kurths J. Enhancing complex-network synchronization. *Europhysics Letters*, 2005, 69: 334-340
[35] Motter A E, Zhou C, Kurths, J. Network synchronization, diffusion, and the paradox of heterogeneity. *Phys. Rev. E*, 2005, 71: 016116
[36] Chavez M, Hwang D-U, Amann A, et al. Synchronization is enhanced in weighted complex networks. *Phys. Rev. Lett.*, 2005, 94: 218701
[37] Kocarev L, Amato P. Synchronization in power-law networks. *Chaos*, 2005, 15: 024101
[38] Fan J, Wang X F. On synchronization in scale-free dynamical networks. *Physica A*, 2005, 349: 443-451
[39] Fan J, Li X, Wang X F. On synchronous preference of complex dynamical networks. *Physica A*, 2005, 355: 657-666
[40] Li X. Uniform synchronous criticality of diversely random complex networks. *Physica A*, 2006, 360: 629-636
[41] Lu W L, Chen T P. New approach to synchronization analysis of linearly coupled ordinary differential equations. *Physics D*, 2006, 213: 214-230
[42] Liu C, Duan Z S, Chen G, Huang L. Synchronization regions in complex networks: analysis and control. *Physica A*, 2007, 386: 531-542
[43] Strogatz S H. From Kuramoto to Crawford: exploring the onset of synchronization in populations of coupled oscillators. *Physica D*, 2000, 143: 1–20
[44] Acebrón, J A, Bonilla L, Vicente C J P et al. The Kuramoto model: A simple paradigm for synchronization phenomena. *Reviews of Modern Physics*, 2005, 77: 137--186
[45] Hong H, Choi M Y, Kim B J. Synchronization on small-world networks. *Phys. Rev. E*, 2002, 65: 026139
[46] Moreno Y, Pacheco A F. Synchronization of Kuramoto oscillators in scale-free

networks, *Europhysics Letters*, 2004, 68: 603-609

[47] Ichinomiya T. Frequency synchronization in random oscillator network. *Phys. Rev. E,* 2004, 70: 026116

[48] Goh K-L, Kahng B, Kim D. Universal behavior of load distribution in scale-free networks. *Phys. Rev. Lett*, 2001, 87: 278701

[49] Lu W, Chen T. New approach to synchronization analysis of linearly coupled ordinary diferential systems. *Physica D*, 2006, 213: 214-230

[50] Duan ZS, Chen G, Huang L. Complex network synchronizability: analysis and control, *Phys. Rev. E*, 2007, 76: 056103 (1-6)

[51] Duan ZS, Chen G, Huang L. Network synchronizability analysis: The theory of subgraphs and complementary graphs. *Physica D*, 2008, 237:1006-1012

[52] Chen G, Duan ZS. Network synchronizability analysis: a graph-theoretic approach.' *Chaos*, 2008, 18: 037102

[53] Boccaletti S, Latora V, Moreno Y, Chavez M, Hwang D U. Complex networks: structure and dynamics. Physics Reports, 2006, 424: 175-308.

[54] Arenas A, Diaz-Guilera A, Kurths J, Moreno Y, Zhou C. Synchronization in complex networks. *Physics Report*, 2008, 469: 93-153

